A Simple Implementation of an Entangler Circuit by Using Quantum Linear Optics

Marco Simonetti[1,2(✉)], Damiano Perri[1,2], and Osvaldo Gervasi[2]

[1] Department of Mathematics and Computer Science, University of Florence, Florence, Italy
[2] Department of Mathematics and Computer Science, University of Perugia, Perugia, Italy
m.simonetti@unifi.it

Abstract. The topic of quantum computing is one that is expanding quickly and has the potential to completely change how some difficult problems can be resolved. In recent years, there has been considerable advancement in the research and application of quantum computing technologies. The use of this technology to address challenging or impractical tasks for conventional computers is an area of ongoing research.

By creating an optical entangler, a quantum-helpful circuit for generating pairs of intensely entangled states, which are useful in numerous applications including quantum teleportation, quantum dense coding, and quantum error correction, this work has demonstrated a potential application of these technologies. Although the Optical Dual Rail Mode has shown to be extremely helpful for scaling up optical quantum circuits, there are still many obstacles and issues that need to be resolved before it can be widely applied in quantum computing.

Keywords: Quantum Computing · Optical Quantum Processing Unit · Entangler · Dual Rail Mode

1 Introduction

Photon chips are one of the most promising platforms for quantum computing. They have several advantages over other physical systems, such as ions or superconducting qubits, that make them particularly suitable for specific quantum computing tasks. Photons' inherent ability to travel long distances without significant loss of coherence is an important advantage. That makes them ideal for use in quantum communication, where quantum information is transmitted over large distances through optical fibres or free-space channels. Photons are already a well-established technology for quantum communication, with several commercial applications such as quantum key distribution and secure transmission. Another benefit of photons is their ability to be manipulated using linear optical devices such as beam splitters, phase shifters, and polarizers.

© The Author(s), under exclusive license to Springer Nature Switzerland AG 2023
O. Gervasi et al. (Eds.): ICCSA 2023 Workshops, LNCS 14104, pp. 116–129, 2023.
https://doi.org/10.1007/978-3-031-37105-9_9

The main difficulty in using photons for quantum computing is their lack of strong interactions with each other. So, to perform entangling operations between two photons, it is necessary to use a non-linear optical element, which is typically weak and hard to control. However, recent advances in materials science have led to the development of new types of non-linear optical materials, such as diamond nitrogen-vacancy centres that can be used to implement high-fidelity two-qubit gates between photons. Another challenge to performing quantum computation with photons is the problem of detecting single photons with high efficiency: it is necessary to detect individual photons with high efficiency reliably. Several technologies for photon detection exist, including single-photon avalanche photodiodes (SPADs) and transition-edge sensors (TESs), but each has its strengths and weaknesses. However, the use of photons in quantum computing has already led to several impressive demonstrations of quantum algorithms, including reduced and simplified versions of Shor's algorithm for factoring large numbers and Grover's algorithm for database search or some applications in Machine Learning.

A Discrete Variable quantum circuit may be implemented using an optical circuit. There are several alternative encodings, such as *spatial modes encoding* and *polarisation modes encoding*. Each qubit in a quantum circuit has a pair of spatial qumodes when using spatial modes encoding. One photon in one of the spatial modes corresponds to each qubit state in a Fock state[1]: so, the quantum state $|0\rangle$ can be encoded as $|1,0\rangle$ in spatial mode, where one photon is in the first qumode, and no photons are in the second one; consequently, the quantum state $|1\rangle$ can be encoded as $|0,1\rangle$. This model is called *Dual Rail Mode*.

In other words, two spatial modes are used to represent each qubit, with one mode corresponding to the logical 0-state (0_L) and the other mode corresponding to the logical 1-state (1_L). The qubit state is then encoded as a superposition of the two spatial modes, with the relative amplitudes of the modes determining the probability of measuring the qubit in the 0 or 1 state [1].

The uses of Quantum Computing, even if the technology is still in its infancy, are remarkable: they have the potential to revolutionize fields such as cryptography, drug discovery, financial modeling, weather forecasting, and optimization problems in logistics and transportation, among others [2–4]. Quantum computers can solve certain complex problems exponentially faster than classical computers, which makes them promising for tasks that require significant computing power [5]. Additionally, quantum computing can enable the development of new technologies such as quantum sensing and quantum communication, which could

[1] The Fock space is a mathematical construction used to describe the quantum states of a system of identical particles, such as electrons, photons, or atoms. It is a Hilbert space that is built up from a vacuum state, which represents the absence of any particles, and a set of creation and annihilation operators, which create and destroy particles. The Fock space is a powerful tool for calculating the probabilities of different quantum states of a system of identical particles.

have significant implications for various industries. While quantum computing is still in its early stages, its potential applications and impact are vast and exciting to consider.

2 Related Works

One of the topics that contributed to the development of quantum computing based on optical properties is the *Quantum Optical Linear Circuit* (QOLC), which is a linear optical circuit that is used to manipulate quantum states of light [6–8]. It is composed of passive linear optical elements, such as beam splitters and phase shifters, and single-photon detectors. The beam splitter and the phase shifter can be described mathematically through a unitary Gaussian matrix. The main components of a QOLC are:

- **Input port**: it is a physical port where the quantum state of light is introduced into the circuit. The input port can be a single-mode or multi-mode fibre, depending on the application; it must be designed to minimise losses and maintain the coherence of the quantum state. A *single photon source* is always present upstream of the input port. During its propagation within the quantum circuit, its distribution wave is processed to enable computation. Single photon sources are defined by specifying parameters such as *brightness*, *purity* or *indistinguishability* [9–11]. The model that describes a single photon source is the perfect/imperfect quantum-dot-based single-photon source obtained by a statistical combination of Fock states.
- **Phase shifters**: they are passive linear optical elements that change the phase of a beam of light. Phase shifters are used to adjust the photon's phase to create interference patterns and manipulate the quantum state of light.
- **Beam splitters**: they are passive linear optical elements that split a beam of light into two or more beams. They are used to separate and recombine photons. By adjusting the reflectivity and transmissivity of the beam splitter, interference patterns can be created to manipulate the quantum state of light. In certain encoding forms, such as Single Photon Mode, they are also used to produce entangled states, a critical resource for quantum communication and quantum computing.
- **Detectors**: they detect the photons that exit the circuit. Single-photon detectors are typically used in QOLC, as they can detect individual photons. They must also be designed to maximise detection efficiency and minimise noise.

The results obtained from the circuit are filtered and sampled according to the methods of Boson Sampling [12–15]. Thanks to VR and Cloud technology advancements [16–21], researchers now have access to valuable resources that allow them to study and gain a deeper understanding of quantum phenomena. They can also experiment and test their ideas on remote platforms that use real quantum processors.

3 The Entangler Circuit in Dual Rail Mode

A quantum optical spatial dual rail circuit is a type of quantum circuit that operates on photons using a spatial encoding scheme called dual-rail encoding. This scheme divides a single photon into two separate spatial modes: the *signal* and *idler* modes. These two modes can be considered two separate paths. The dual rail encoding scheme helps to perform quantum computations because it allows for the encoding of quantum information in a robust way against certain types of errors. For example, the dual rail encoding can be used to encode a qubit, where the presence or absence of a photon in the signal mode represents the logical state $|0\rangle_L$, and the presence or absence of a photon in the idler mode means the logical state $|1\rangle_L$.

So, in this specific case, the state $|1,0\rangle$ has been chosen for logic state $|0\rangle_L$ and the state $|0,1\rangle$ for logic state $|1\rangle_L$. In this work, we present the circuit implementation of an Entangler (Fig. 1, Eq. 1), helpful in generating Bell's states [22–24].

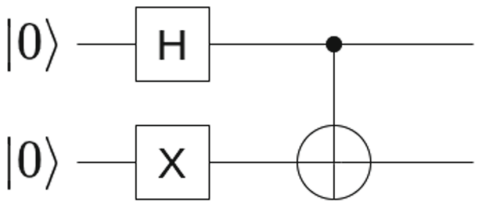

Fig. 1. Entangler Circuit

$$
\begin{aligned}
|\psi_{out}\rangle &= CX \cdot \big(H \otimes X\big) \cdot |00\rangle = \\
&= \big(|0\rangle\langle 0| \otimes \mathbb{I} + |1\rangle\langle 1| \otimes X\big) \cdot \big(H \otimes X\big) \cdot |00\rangle = \\
&= \big(|0\rangle\langle 0| \otimes \mathbb{I} + |1\rangle\langle 1| \otimes X\big) \cdot \big(H \otimes X\big) \cdot (|0\rangle \otimes |0\rangle) = \\
&= \big(|0\rangle\langle 0| \otimes \mathbb{I} + |1\rangle\langle 1| \otimes X\big) \cdot \big(H|0\rangle \otimes X|0\rangle\big) = \\
&= \big(|0\rangle\langle 0| \otimes \mathbb{I} + |1\rangle\langle 1| \otimes X\big) \cdot \frac{1}{\sqrt{2}}\big((|0\rangle + |1\rangle) \otimes |1\rangle\big) = \\
&= \frac{1}{\sqrt{2}}\big(|0\rangle\,\langle 0|0\rangle + |0\rangle\,\langle 0|1\rangle\big) \otimes \big(\mathbb{I}|1\rangle\big) + \\
&+ \frac{1}{\sqrt{2}}\big(|1\rangle\,\langle 1|0\rangle + |1\rangle\,\langle 1|1\rangle\big) \otimes \big(X|1\rangle\big) = \\
&= \frac{1}{\sqrt{2}}\big(|0\rangle \otimes |1\rangle\big) + \frac{1}{\sqrt{2}}\big(|1\rangle \otimes |0\rangle\big) = \frac{1}{\sqrt{2}}|01\rangle + \frac{1}{\sqrt{2}}|10\rangle
\end{aligned}
\tag{1}
$$

The first stage of the entangler, i.e. $H \otimes X$, can be implemented as in Fig. 2, having got their equivalent representation utilising a beam splitter and four phase shifters to constitute gates H and X; that is possible employing some unit matrix decomposition schemes [25–28]. This section will present the circuit implementation of an Entangler [29–32] using linear quantum optics. The circuit was built and tested with the Perceval software[2] [33], and the results obtained were later compared with the outcome got from a true quantum optical computer in the cloud, Quandela Cloud[3]. Consequently, for displaying the various gates in the circuit, the graphical and mathematical conventions given by the software are followed[4].

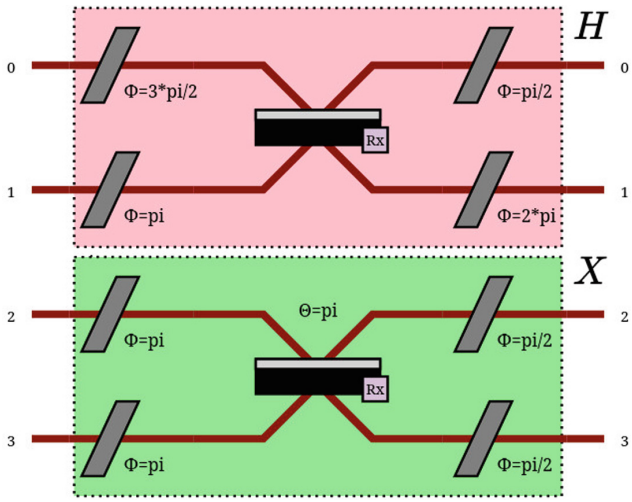

Fig. 2. Optical equivalent gates: H (in pink) and X (in green) (Color figure online)

Relating to the implementation of CNOT, it is essential to empathise that, in dual-rail encoding, deterministic two-qubit gates are impossible, and a chance of failure always exists. This nonsuccess can be detected in two ways: by using additional photons, known as *ancillas*, that are measured independently from the information photons to determine if the gate was successful on the information qubits (these gates are known as *heralded*); or by directly measuring the information qubits and assessing whether the gate was successful based on the result (these gates are known as *postselected*). The CNOT gate operates on two qubits (two couples of modes), a *control* and a *target*, and inverts the value of the target if the control qubit is in the logical state $|1\rangle_L$. Two types of CNOT gates occur most in the literature: the **postselected CNOT** of Ralph [34] and the **heralded CNOT** of the KLM (Knill-Laflamme-Milburn) protocol [35].

[2] https://perceval.quandela.net/docs/index.html.
[3] https://cloud.quandela.com/webide/login.
[4] https://perceval.quandela.net/docs/components.html.

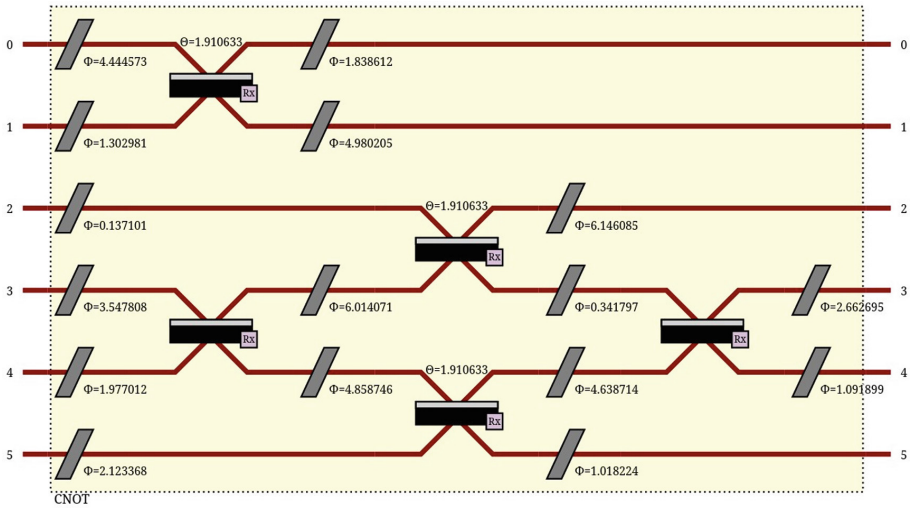

Fig. 3. Proposed Optical CNOT schema

A CNOT gate of the first type, which is less sophisticated but much more straightforward to build than the other one, is sufficient to implement the proposed entangler circuit (Fig. 3 and Fig. 4). On the Entangler in Fig. 4, however, it is possible to operate some significant simplifications, which help to make the physical realisation of the circuit easier and reduce noise due to unnecessary additional components. An optical Entangler like the one in Fig. 5 is therefore proposed. Some useful tools provided by the simulation software allow one to verify the equivalence between the circuits in Fig. 4 and Fig. 5: both have the same unitary matrix (Eq. 2).

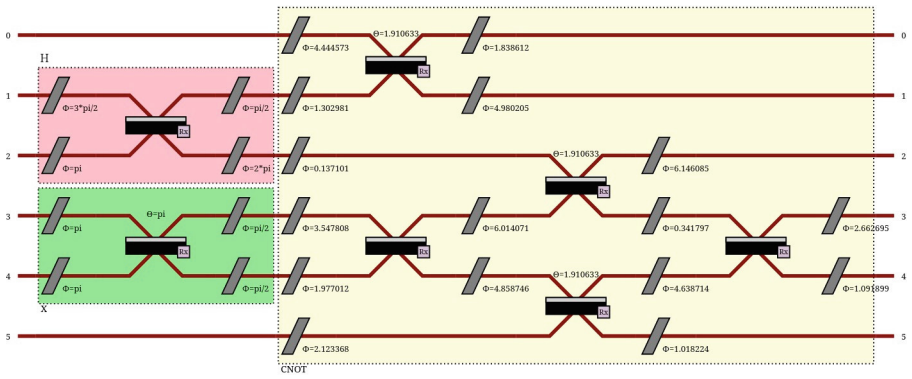

Fig. 4. Entangler built from the two previous blocks

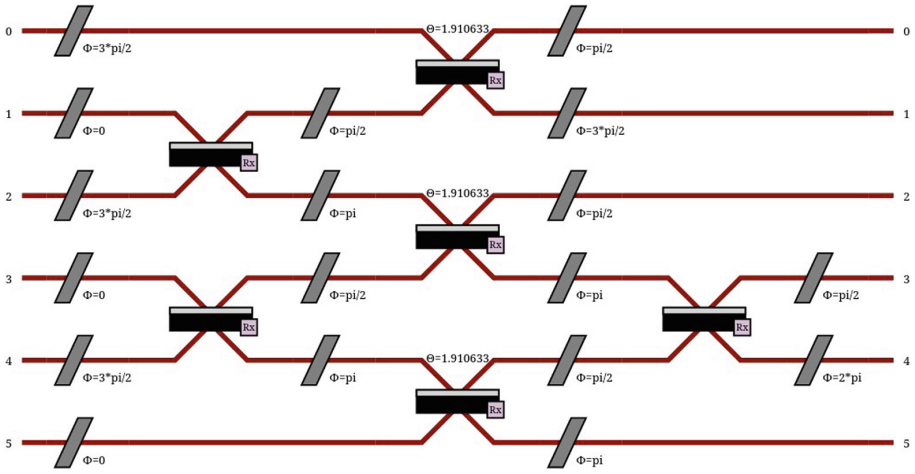

Fig. 5. Simplified proposed Entangler

$$U = \begin{pmatrix} \frac{\sqrt{3}}{3} & -\frac{\sqrt{3}i}{3} & -\frac{\sqrt{3}i}{3} & 0 & 0 & 0 \\ -\frac{\sqrt{6}i}{3} & \frac{\sqrt{6}}{6} & \frac{\sqrt{6}}{6} & 0 & 0 & 0 \\ 0 & \frac{\sqrt{6}}{6} & -\frac{\sqrt{6}}{6} & -\frac{\sqrt{3}i}{3} & -\frac{\sqrt{3}i}{3} & 0 \\ 0 & -\frac{\sqrt{6}i}{6} & \frac{\sqrt{6}i}{6} & 0 & \frac{\sqrt{3}}{3} & \frac{\sqrt{3}}{3} \\ 0 & -\frac{\sqrt{6}i}{6} & \frac{\sqrt{6}i}{6} & \frac{\sqrt{3}}{3} & 0 & -\frac{\sqrt{3}}{3} \\ 0 & 0 & 0 & -\frac{\sqrt{3}}{3} & \frac{\sqrt{3}}{3} & -\frac{\sqrt{3}}{3} \end{pmatrix} \tag{2}$$

Modes labelled 0 and 5 are the ancillary modes. No photons are provided into them; the output state is guaranteed to be correct only if no photons are detected on the output stage of ancillary modes after a measurement process. The modes labelled 1,2 and 3,4 encode the two classical input qubits $|0\rangle \otimes |0\rangle = |00\rangle$, respectively; further, $|0\rangle$ is $|1,0\rangle$ and $|1\rangle$ is $|0,1\rangle$. That means the input state $|\psi_{in}\rangle$ is $|0,1,0,1,0,0\rangle$, with

$$|\psi_{in}\rangle = |\overbrace{0}^{ancilla}, \overbrace{1,\ 0}^{qubit_1}, \overbrace{1,\ 0}^{qubit_0}, \overbrace{0}^{ancilla}\rangle$$

From Eq. 2, it results that the annihilation operators describing the relationships between the input and the output of the circuit are related by the following expressions

$$
\begin{pmatrix} \hat{b}_0 \\ \hat{b}_1 \\ \hat{b}_2 \\ \hat{b}_3 \\ \hat{b}_4 \\ \hat{b}_5 \end{pmatrix} = \begin{pmatrix} \frac{\sqrt{3}}{3} & -\frac{\sqrt{3}i}{3} & -\frac{\sqrt{3}i}{3} & 0 & 0 & 0 \\ -\frac{\sqrt{6}i}{3} & \frac{\sqrt{6}}{6} & \frac{\sqrt{6}}{6} & 0 & 0 & 0 \\ 0 & \frac{\sqrt{6}}{6} & -\frac{\sqrt{6}}{6} & -\frac{\sqrt{3}i}{3} & -\frac{\sqrt{3}i}{3} & 0 \\ 0 & -\frac{\sqrt{6}i}{6} & \frac{\sqrt{6}i}{6} & 0 & \frac{\sqrt{3}}{3} & \frac{\sqrt{3}}{3} \\ 0 & -\frac{\sqrt{6}i}{6} & \frac{\sqrt{6}i}{6} & \frac{\sqrt{3}}{3} & 0 & -\frac{\sqrt{3}}{3} \\ 0 & 0 & 0 & -\frac{\sqrt{3}}{3} & \frac{\sqrt{3}}{3} & -\frac{\sqrt{3}}{3} \end{pmatrix} \cdot \begin{pmatrix} \hat{a}_0 \\ \hat{a}_1 \\ \hat{a}_2 \\ \hat{a}_3 \\ \hat{a}_4 \\ \hat{a}_5 \end{pmatrix}
$$

$$
\begin{pmatrix} \hat{a}_0^\dagger \\ \hat{a}_1^\dagger \\ \hat{a}_2^\dagger \\ \hat{a}_3^\dagger \\ \hat{a}_4^\dagger \\ \hat{a}_5^\dagger \end{pmatrix} = \begin{pmatrix} \frac{\sqrt{3}}{3} & -\frac{\sqrt{6}i}{3} & 0 & 0 & 0 & 0 \\ -\frac{\sqrt{3}i}{3} & \frac{\sqrt{6}}{6} & \frac{\sqrt{6}}{6} & -\frac{\sqrt{6}i}{6} & -\frac{\sqrt{6}i}{6} & 0 \\ -\frac{\sqrt{3}i}{3} & \frac{\sqrt{6}}{6} & -\frac{\sqrt{6}}{6} & \frac{\sqrt{6}i}{6} & \frac{\sqrt{6}i}{6} & 0 \\ 0 & 0 & -\frac{\sqrt{3}i}{3} & 0 & \frac{\sqrt{3}}{3} & -\frac{\sqrt{3}}{3} \\ 0 & 0 & -\frac{\sqrt{3}i}{3} & \frac{\sqrt{3}}{3} & 0 & \frac{\sqrt{3}}{3} \\ 0 & 0 & 0 & \frac{\sqrt{3}}{3} & -\frac{\sqrt{3}}{3} & -\frac{\sqrt{3}}{3} \end{pmatrix} \cdot \begin{pmatrix} \hat{b}_0^\dagger \\ \hat{b}_1^\dagger \\ \hat{b}_2^\dagger \\ \hat{b}_3^\dagger \\ \hat{b}_4^\dagger \\ \hat{b}_5^\dagger \end{pmatrix} \tag{3}
$$

Equations 3 and 4 show the procedure for calculating the output state, starting from the initial state. That will allow comparing the correctness of the results obtained with the simulator and with the real optical quantum computer.

$$
\begin{cases}
\hat{a}_0^\dagger = \frac{\sqrt{3}}{3}\hat{b}_0^\dagger - \frac{\sqrt{6}i}{3}\hat{b}_1^\dagger \\
\hat{a}_1^\dagger = -\frac{\sqrt{3}i}{3}\hat{b}_0^\dagger + \frac{\sqrt{6}}{6}\hat{b}_1^\dagger + \frac{\sqrt{6}}{6}\hat{b}_2^\dagger - \frac{\sqrt{6}i}{6}\hat{b}_3^\dagger - \frac{\sqrt{6}i}{6}\hat{b}_4^\dagger \\
\hat{a}_2^\dagger = -\frac{\sqrt{3}i}{3}\hat{b}_0^\dagger + \frac{\sqrt{6}}{6}\hat{b}_1^\dagger - \frac{\sqrt{6}}{6}\hat{b}_2^\dagger + \frac{\sqrt{6}i}{6}\hat{b}_3^\dagger + \frac{\sqrt{6}i}{6}\hat{b}_4^\dagger \\
\hat{a}_3^\dagger = -\frac{\sqrt{3}i}{3}\hat{b}_2^\dagger + \frac{\sqrt{3}}{3}\hat{b}_4^\dagger - \frac{\sqrt{3}}{3}\hat{b}_5^\dagger \\
\hat{a}_4^\dagger = -\frac{\sqrt{3}i}{3}\hat{b}_2^\dagger + \frac{\sqrt{3}}{3}\hat{b}_3^\dagger + \frac{\sqrt{3}}{3}\hat{b}_5^\dagger \\
\hat{a}_5^\dagger = \frac{\sqrt{3}}{3}\hat{b}_3^\dagger - \frac{\sqrt{3}}{3}\hat{b}_4^\dagger - \frac{\sqrt{3}}{3}\hat{b}_5^\dagger
\end{cases} \tag{4}
$$

$$|0,1,0,1,0,0\rangle = \hat{a}_1^\dagger \hat{a}_3^\dagger |0,0,0,0,0,0\rangle$$

$$\hat{a}_1^\dagger \hat{a}_3^\dagger = \left(-\frac{\sqrt{3}i}{3}\hat{b}_0^\dagger + \frac{\sqrt{6}}{6}\hat{b}_1^\dagger + \frac{\sqrt{6}}{6}\hat{b}_2^\dagger - \frac{\sqrt{6}i}{6}\hat{b}_3^\dagger - \frac{\sqrt{6}i}{6}\hat{b}_4^\dagger\right)\left(-\frac{\sqrt{3}i}{3}\hat{b}_2^\dagger + \frac{\sqrt{3}}{3}\hat{b}_4^\dagger - \frac{\sqrt{3}}{3}\hat{b}_5^\dagger\right)$$

$$= \left(-\frac{1}{3}\hat{b}_0^\dagger\hat{b}_2^\dagger - \frac{i}{3}\hat{b}_0^\dagger\hat{b}_4^\dagger + \frac{i}{3}\hat{b}_0^\dagger\hat{b}_5^\dagger - \frac{\sqrt{2}i}{6}\hat{b}_1^\dagger\hat{b}_2^\dagger + \frac{\sqrt{2}}{6}\hat{b}_1^\dagger\hat{b}_4^\dagger - \frac{\sqrt{2}}{6}\hat{b}_1^\dagger\hat{b}_5^\dagger - \frac{\sqrt{2}i}{6}\hat{b}_2^{\dagger 2} + \right.$$
$$\left. - \frac{\sqrt{2}}{6}\hat{b}_2^\dagger\hat{b}_3^\dagger - \frac{\sqrt{2}}{6}\hat{b}_2^\dagger\hat{b}_5^\dagger - \frac{\sqrt{2}i}{6}\hat{b}_3^\dagger\hat{b}_4^\dagger + \frac{\sqrt{2}i}{6}\hat{b}_3^\dagger\hat{b}_5^\dagger - \frac{\sqrt{2}i}{6}\hat{b}_4^{\dagger 2} + \frac{\sqrt{2}i}{6}\hat{b}_4^\dagger\hat{b}_5^\dagger\right)$$

$$|\psi_{out}\rangle = \hat{a}_1^\dagger \hat{a}_3^\dagger |0,0,0,0,0,0\rangle =$$
$$= -\frac{1}{3}b_0^\dagger b_2^\dagger|0,0,0,0,0,0\rangle - \frac{i}{3}b_0^\dagger b_4^\dagger|0,0,0,0,0,0\rangle + \frac{i}{3}b_0^\dagger b_5^\dagger|0,0,0,0,0,0\rangle +$$
$$- \frac{\sqrt{2}i}{6}b_1^\dagger b_2^\dagger|0,0,0,0,0,0\rangle + \frac{\sqrt{2}}{6}b_1^\dagger b_4^\dagger|0,0,0,0,0,0\rangle - \frac{\sqrt{2}}{6}b_1^\dagger b_5^\dagger|0,0,0,0,0,0\rangle +$$
$$- \frac{\sqrt{2}i}{6}{b_2^\dagger}^2|0,0,0,0,0,0\rangle - \frac{\sqrt{2}}{6}b_2^\dagger b_3^\dagger|0,0,0,0,0,0\rangle - \frac{\sqrt{2}}{6}b_2^\dagger b_5^\dagger|0,0,0,0,0,0\rangle +$$
$$- \frac{\sqrt{2}i}{6}b_3^\dagger b_4^\dagger|0,0,0,0,0,0\rangle + \frac{\sqrt{2}i}{6}b_3^\dagger b_5^\dagger|0,0,0,0,0,0\rangle - \frac{\sqrt{2}i}{6}{b_4^\dagger}^2|0,0,0,0,0,0\rangle +$$
$$+ \frac{\sqrt{2}i}{6}b_4^\dagger b_5^\dagger|0,0,0,0,0,0\rangle$$

Now applying the creation operators $\hat{b}_i^\dagger$ to the appropriate mode i-th of the vector $|0,0,0,0,0,0\rangle$, we obtain the output state of the optical quantum system under consideration:

$$\begin{aligned}|\psi_{out}\rangle &= \hat{a}_1^\dagger \hat{a}_3^\dagger |0,0,0,0,0,0\rangle = \\ &= -\frac{1}{3}|1,0,1,0,0,0\rangle - \frac{i}{3}|1,0,0,0,1,0\rangle + \frac{i}{3}|1,0,0,0,0,1\rangle + \\ &- \frac{\sqrt{2}i}{6}|0,1,1,0,0,0\rangle + \frac{\sqrt{2}}{6}|0,1,0,0,1,0\rangle - \frac{\sqrt{2}}{6}|0,1,0,0,0,1\rangle + \\ &- \frac{i}{3}|0,0,2,0,0,0\rangle - \frac{\sqrt{2}}{6}|0,0,1,1,0,0\rangle - \frac{\sqrt{2}}{6}|0,0,1,0,0,1\rangle + \\ &- \frac{\sqrt{2}i}{6}|0,0,0,1,1,0\rangle + \frac{\sqrt{2}i}{6}|0,0,0,1,0,1\rangle - \frac{i}{3}|0,0,0,0,2,0\rangle + \\ &+ \frac{\sqrt{2}i}{6}|0,0,0,0,1,1\rangle\end{aligned} \tag{5}$$

The space dimension describing this transformation is given by the formula $C_n^{m+n-1} = \binom{m+n-1}{n}$, where m is the number of modes in system and n is the number of photons in input; here, the dimension is $\binom{6+3-1}{3} = 21$: the components of the state vector given by Eq. 5 have only 13 non-zero probability amplitudes, while the remaining eight are zero.

Since modes 0 and 5 are heralded (it means 0 photons in them, 0 photons expected out of them), the output state $|\psi_{out}\rangle$ collapses after a measurement process and the relative filtering step to eliminate all the states with mode 0 or mode 5 different from zero; the new output state consequently becomes $|\psi'_{out}\rangle$ (in order to improve readability, the ancillary states have been omitted).

$$|\psi'_{out}\rangle = -\frac{\sqrt{2}i}{4}|1,1,0,0\rangle + \frac{\sqrt{2}}{4}|1,0,0,1\rangle - \frac{i}{2}|0,2,0,0\rangle - \frac{\sqrt{2}}{4}|0,1,1,0\rangle - \frac{\sqrt{2}i}{4}|0,0,1,1\rangle - \frac{i}{2}|0,0,0,2\rangle \tag{6}$$

Subsequently, because the modes encoding the individual qubits can only contain a single photon alternatively, all those states that do not respect this constraint are discarded. The final state remaining after this post-selection operation, hence, results $|\psi''_{out}\rangle$.

$$|\psi''_{out}\rangle = +\frac{\sqrt{2}}{2}|1,0,0,1\rangle - \frac{\sqrt{2}}{2}|0,1,1,0\rangle \tag{7}$$

The outcome is correct because the final state is a Bell's state, as expected. So, output outcomes for probability distribution for the state in $|\psi''_{out}\rangle$ are $\frac{1}{2}$ for the state $|1,0,0,1\rangle$ and $\frac{1}{2}$ for the state $|0,1,1,0\rangle$. Circuit simulations with Perceval (Table 1, Fig. 6, Fig. 7 and Fig. 8) show perfect agreement with the theoretically obtained results.

Table 1. Probability of each state composing final output state for the Dual Rail Entangler with input $|0,1,0,1,0,0\rangle$; results obtained with Perceval.

state	probability
$\|1,0,1,0,0,0\rangle$	0.111111
$\|2,0,0,0,0,0\rangle$	0.000000
$\|1,0,0,0,1,0\rangle$	0.111111
$\|0,2,0,0,0,0\rangle$	0.000000
$\|0,1,0,1,0,0\rangle$	0.000000
$\|0,0,0,1,0,1\rangle$	0.055556
$\|0,0,0,0,2,0\rangle$	0.111111
$\|0,1,0,0,0,1\rangle$	0.055556
$\|0,0,1,0,1,0\rangle$	0.000000
$\|0,0,0,2,0,0\rangle$	0.000000
$\|0,0,0,0,0,2\rangle$	0.000000
$\|1,1,0,0,0,0\rangle$	0.000000
$\|1,0,0,1,0,0\rangle$	0.000000
$\|1,0,0,0,0,1\rangle$	0.111111
$\|0,1,1,0,0,0\rangle$	0.055556
$\|0,1,0,0,1,0\rangle$	0.055556
$\|0,0,1,0,0,1\rangle$	0.055556
$\|0,0,0,1,1,0\rangle$	0.055556
$\|0,0,1,1,0,0\rangle$	0.055556
$\|0,0,0,0,1,1\rangle$	0.055556
$\|0,0,2,0,0,0\rangle$	0.111111

```
Initial State: |0,1,0,1,0,0>
---------------------------------------------------------------
Ouput State:
|1,0,1,0,0,0> (-0.3333333333333333-1.263373392013101e-09j)
|1,0,0,0,1,0> (8.603854712019301e-10-0.33333333333333337j)
|1,0,0,0,0,1> (-3.7847472817382997e-10+0.3333333333333334j)
|0,1,1,0,0,0> (8.917603877556248e-10-0.23570226039551578j)
|0,1,0,0,1,0> (0.23570226039551584+6.068048979956943e-10j)
|0,1,0,0,0,1> (-0.23570226039551584-2.66042558938492e-10j)
|0,0,2,0,0,0> (7.459158944326773e-11-0.33333333333333315j)
|0,0,1,1,0,0> (-0.23570226039551584+7.985322125758645e-10j)
|0,0,1,0,0,1> (-0.23570226039551578+5.72973640755592e-10j)
|0,0,0,1,1,0> (-9.62582347163732e-10-0.23570226039551578j)
|0,0,0,1,0,1> (1.363797379137784e-09+0.23570226039551584j)
|0,0,0,0,2,0> (-6.458912113628097e-10-0.33333333333333326j)
|0,0,0,0,1,1> (7.974764182350216e-10+0.23570226039551584j)

-1/3*|1,0,1,0,0,0>
-I/3*|1,0,0,0,1,0>
+I/3*|1,0,0,0,0,1>
-sqrt(2)*I/6*|0,1,1,0,0,0>
+sqrt(2)/6*|0,1,0,0,1,0>
-sqrt(2)/6*|0,1,0,0,0,1>
-I/3*|0,0,2,0,0,0>
-sqrt(2)/6*|0,0,1,1,0,0>
-sqrt(2)/6*|0,0,1,0,0,1>
-sqrt(2)*I/6*|0,0,0,1,1,0>
+sqrt(2)*I/6*|0,0,0,1,0,1>
-I/3*|0,0,0,0,2,0>
+sqrt(2)*I/6*|0,0,0,0,1,1>
---------------------------------------------------------------
```

Fig. 6. Output state from simulation on Perceval of Dual-Rail Entangler Circuit

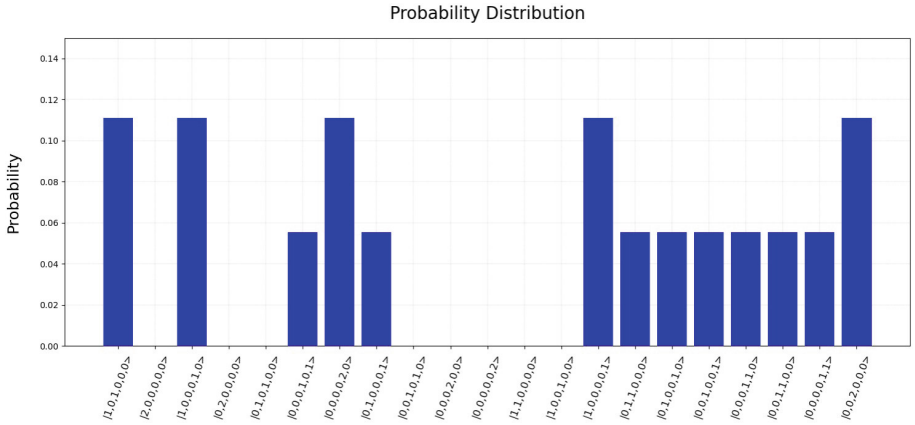

Fig. 7. Probability distribution for state $|\psi_{out}\rangle$ on Perceval of Dual-Rail Entangler Circuit

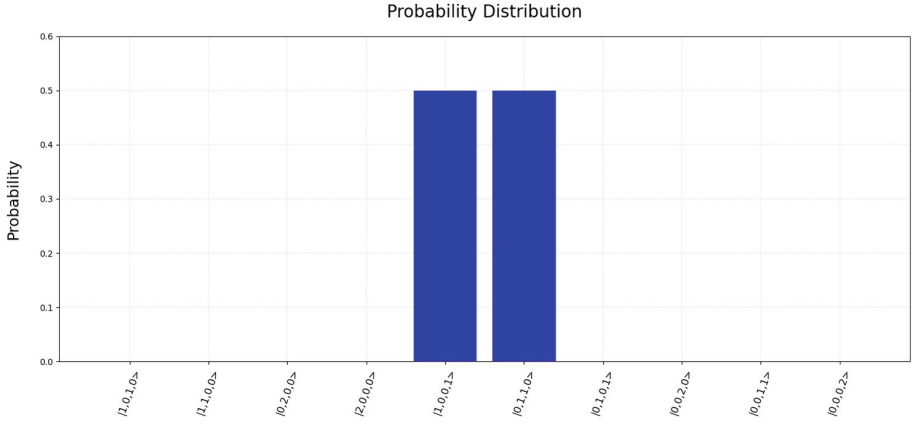

Fig. 8. Probability distribution for state $|\psi''_{out}\rangle$ on Perceval of Dual-Rail Entangler Circuit

4 Conclusions

Quantum computing is a rapidly growing area that has the potential to revolutionise the way some complex problems can be solved. The development and usage of quantum computing technology have made significant progress in recent years. Researchers are continuously exploring new ways to leverage this technology to solve complex or impossible problems for classical computers. Quantum computing's unique properties, such as superposition and entanglement, enable it to perform specific calculations exponentially faster than classical computers.

This paper has illustrated a possible application of these technologies by realizing an optical entangler, a quantum helpful circuit for producing pairs of maximally entangled states intensely used in many applications such as quantum

teleportation, quantum dense coding and quantum error correction. The Optical Dual Rail Mode has proved to be very useful for scaling up optical quantum circuits but still has many challenges and problems to be solved to be widely used in quantum computing.

We intend to deepen this line of studies in successive works, especially by implementing quantum algorithms using linear and non-linear optics.

References

1. Isaac, L.: Chuang and Yoshihisa Yamamoto. Simple quantum computer. Phys. Rev. A **52**(5), 3489 (1995)
2. Simonetti, M., Perri, D., Gervasi, O.: An example of use of variational methods in quantum machine learning. In: Gervasi, O., Murgante, B., Misra, S., Rocha, A.M.A.C., Garau, C. (eds.) Computational Science and Its Applications –ICCSA 2022 Workshops. ICCSA 2022. LNCS, vol. 13382, pp. 597–609. Springer, Cham (2022). https://doi.org/10.1007/978-3-031-10592-0_43
3. Abdelgaber, N., Nikolopoulos, C.: Overview on quantum computing and its applications in artificial intelligence. In: 2020 IEEE Third International Conference on Artificial Intelligence and Knowledge Engineering (AIKE), pp. 198–199. IEEE (2020)
4. Bayerstadler, A., et al.: Industry quantum computing applications. EPJ Quantum Technol. **8**(1), 25 (2021)
5. Möller, M., Vuik, C.: On the impact of quantum computing technology on future developments in high-performance scientific computing. Ethics Inf. Technol. **19**, 253–269 (2017)
6. Fox, A.M., Fox, M.: Quantum Optics: An Introduction, vol. 15. Oxford University Press, Oxford (2006)
7. Cerf, N.J., Adami, C., Kwiat, P.G.: Optical simulation of quantum logic. Phys. Rev. A **57**(3), R1477 (1998)
8. Ralph, T.C.: Quantum optical systems for the implementation of quantum information processing. Rep. Progress Phys. **69**(4), 853 (2006)
9. Somaschi, N., et al.: Near-optimal single-photon sources in the solid state. Nat. Photonics **10**(5), 340–345 (2016)
10. Ollivier, H., et al.: Reproducibility of highperformance quantum dot single-photon sources. ACS Photonics **7**(4), 1050–1059 (2020)
11. Loredo, J.C., et al. Scalable performance in solid-state single-photon sources. Optica **3**(4), 433–440 (2016)
12. Tillmann, M., Dakić, B., Heilmann, R., Nolte, S., Szameit, A., Walther, P.: Experimental boson sampling. Nat. Photonics **7**(7), 540–544 (2013)
13. Hamilton, C.S., Kruse, R., Sansoni, L., Barkhofen, S., Silberhorn, C., Jex, I.: Gaussian boson sampling. Phys. Rev. Lett. **119**(17), 170501 (2017)
14. Spring, J.B., et al.: Boson sampling on a photonic chip. Science **339**(6121), 798–801 (2013)
15. Brod, D.J., Galvão, E.F., Crespi, A., Osellame, R., Spagnolo, N., Sciarrino, F.: Photonic implementation of boson sampling: a review. Adv. Photonics **1**(3), 034001 (2019)
16. Perri, D., Simonetti, M., Gervasi, O.: Deploying efficiently modern applications on cloud. Electronics **11**(3) (2022). ISSN: 2079-9292. https://doi.org/10.3390/electronics11030450. https://www.mdpi.com/2079-9292/11/3/450

17. Perri, D., Simonetti, M., Tasso, S., Ragni, F., Gervasi, O.: Implementing a scalable and elastic computing environment based on cloud containers. In: Gervasi, O., et al. (eds.) ICCSA 2021. LNCS, vol. 12949, pp. 676–689. Springer, Cham (2021). https://doi.org/10.1007/978-3-030-86653-2_49 ISBN: 978-3-030-86653-2
18. Perri, D., Simonetti, M., Gervasi, O.: Synthetic data generation to speed-up the object recognition pipeline. Electronics **11**(1) (2022). ISSN: 2079-9292. https://doi.org/10.3390/electronics11010002. https://www.mdpi.com/2079-9292/11/1/2
19. Perri, D., Fortunelli, M., Simonetti, M., Magni, R., Carloni, J., Gervasi, O.: Rapid prototyping of virtual reality cognitive exercises in a tele-rehabilitation context. Electronics **10**(4) (2021). ISSN: 2079-9292. https://doi.org/10.3390/electronics10040457. https://www.mdpi.com/2079-9292/10/4/457
20. Perri, D., Simonetti, M., Lombardi, A., Faginas-Lago, N., Gervasi, O.: Binary classification of proteins by a machine learning approach. In: Gervasi, O., et al. (eds.) ICCSA 2020. LNCS, vol. 12255, pp. 549–558. Springer, Cham (2020). ISBN: 978-3-030-58820-5. https://doi.org/10.1007/978-3-030-58820-5_41
21. Laganà, A., Gervasi, O., Tasso, S., Perri, D., Franciosa, F.: The ECTN virtual education community prosumer model for promoting and assessing chemical knowledge. In: Gervasi, O., et al. (eds.) ICCSA 2018. LNCS, vol. 10964, pp. 533–548. Springer, Cham (2018). ISBN: 978-3-319-95174-4. https://doi.org/10.1007/978-3-319-95174-4_42
22. Mermin, N.D.: Hidden variables and the two theorems of john bell. Rev. Mod. Phys. **65**(3), 803 (1993)
23. Zeilinger, A.: Experiment and the foundations of quantum physics. Rev. Mod. Phys. **71**(2), S288 (1999)
24. Lee, H.-W., Kim, J.: Quantum teleportation and Bell's inequality using single-particle entanglement. Phys. Rev. A **63**(1), 012305 (2000)
25. Clements, W.R., Humphreys, P.C., Metcalf, B.J., Kolthammer, W.S.. Walmsley, I.A.: Optimal design for universal multiport interferometers. Optica **3**(12), 1460–1465 (2016)
26. Reck, M., Zeilinger, A., Bernstein, H.J., Bertani, P.: Experimental realization of any discrete unitary operator. Phys. Rev. Lett. **73**(1), 58 (1994)
27. de Guise, H., Di Matteo, O., Sánchez-Soto, L.L.: Simple factorization of unitary transformations. Phys. Rev. A **97**(2), 022328 (2018)
28. Kumar, S.P., Dhand, I.: Unitary matrix decompositions for optimal and modular linear optics architectures. J. Phys. A Math. Theor. **54**(4), 045301 (2021)
29. Imre, S., Balazs, F.: Quantum Computing and Communications: An Engineering Approach. John Wiley & Sons, Hoboken (2005)
30. Asbóth, J.K., Calsamiglia, J., Ritsch, H.: Computable measure of nonclassicality for light. Phys. Rev. Lett. **94**(17), 173602 (2005)
31. Rezakhani, A.T.: Characterization of two-qubit perfect entanglers. Phys. Rev. A **70**(5), 052313 (2004)
32. Zhang, J., Vala, J., Sastry, S., Whaley, K.B.: Geometric theory of nonlocal two-qubit operations. Phys. Rev. A **67**(4), 042313 (2003)
33. Heurtel, N., et al.: Perceval: a software platform for discrete variable photonic quantum computing. Quantum **7**, 931 (2023). ISSN : 2521–327X. https://doi.org/10.22331/q-2023-02-21-931
34. Ralph, T.C., Langford, N.K., Bell, T.B., White, A.G.: Linear optical controlled-NOT gate in the coincidence basis. Phys. Rev. A **65**(6), 062324 (2002)
35. Knill, E., Laflamme, R., Milburn, G.J.: A scheme for efficient quantum computation with linear optics. Nature **409**(6816), 46–52 (2001)